Journal of Applied Polymer Science

Preparation of 2-(dimethylamino) ethyl methacrylate copolymer micelles for shape memory materials

Yan Yang, Funian Mo, Yangyang Chen, Yingyi Liu, Shaojun Chen, Jiandong Zuo
Shenzhen Key Laboratory of Special Functional Materials, Nanshan District Key Lab for Biopolymers and Safety Evaluation, College of Materials Science and Engineering, Shenzhen University, Shenzhen 518060, China
Yan Yang and Funian Mo contributed equally to this work.
Correspondence to: S.J. Chen (E-mail: chensj@szu.edu.cn) and J.D. Zuo (E-mail: jdzuo@szu.edu.cn)

ABSTRACT: Researchers are actively developing shape memory polymers (SMPs) for smart biomaterials. This paper reports a new SMP system synthesized from biocompatible 2-(dimethylamino) ethyl methacrylate (DMAEMA), butyl acrylate (BA) and tri(ethylene glycol) divinyl ether (TDE). Preliminary results show that the DMAEMA-co-BA-co-TDE copolymers form micelles in aqueous solution due to chemical crosslinking and hydrophobicity. The micelle size decreased with the increase in the BA content since the hydrophobicity of copolymers increases with the increase of BA content. The resulting polymer films contain–$N(CH_3)_2$ functional groups for further biomaterial applications. The thermal stability of DMAEMA-co-BA-co-TDE copolymers is determined by the DMAEMA structure and content. Moreover, the copolymers form micro-phase-separated structures containing a reversible amorphous soft phase, and the storage moduli decreases significantly around T_g. Therefore, good thermal-induced shape memory effects are achieved in the DMAEMA-co-BA-co-TDE copolymers by adjusting the BA content. This work proposes a new strategy for designing smart biomaterials using a biocompatible monomer. © 2015 Wiley Periodicals, Inc. J. Appl. Polym. Sci. **2015**, *132*, 42312.

KEYWORDS: 2-(dimethylamino) ethyl methacrylate; biocompatible; biomaterials; micelles; shape memory polymers

Received 19 January 2015; accepted 5 April 2015
DOI: 10.1002/app.42312

INTRODUCTION

Shape memory polymers (SMPs) have received significant attention in recent years because they have the capability of fixing a temporary shape and recovering their original shape upon the application of an external stimulus.[1,2] These polymers show tremendous potential in the fields of biotechnology, biomaterials and polymer processing. For biomedical applications, SMPs should also be biocompatible and have tunable actuation temperatures and glassy elastic moduli.[3,4] Biocompatible SMPs have thus attracted increasing attention from researchers. Many types of SMPs, including Diapplex shape memory polyurethanes (SMPUs), polylactic acid (PLA)-SMPUs and polycaprolactone (PCL)-diacrylate SMPs, are reported to have good biocompatibility, as demonstrated by low cytotoxicity, low thrombogenicity, low platelet activation, low cytokine activation and low *in vivo* inflammatory response.[3,4] However, to date, only a few SMP-based biomedical devices have been commercialized. Thus, it is of great urgency to develop more biocompatible SMPs.

It is well known that poly(2-(dimethylamino)ethyl methacrylate) (pDMAEMA) is widely used as a biomaterials double hydrophilic copolymer and environmentally sensitive coating due to its unique chemical structure containing–$N(CH_3)_2$ functional groups, which can be further quaternized or betainized.[5] The literature reveals that the functional monomer 2-(dimethylamino)ethyl methacrylate (DMAEMA) has been widely used to design stimuli-responsive hydrogels,[6,7] micelles,[8–10] brushes,[11–13] and other functional membranes grafted onto various substrates.[14,15] In addition to their responsiveness to pH and temperature,[14–17] DMAEMA-based copolymers can also respond to external stimuli such as ion strength, selected ions and other factors in solution.[5,18] Recently, pDMAEMA has also demonstrated great potential as an ideal carrier for drug delivery or gene delivery because of its relatively low toxicity and high transfection efficiency.[19] However, to the best of our knowledge, shape memory functionalities have not been reported in DMAEMA-based copolymers. Based on their structure, these polymers are expected to show multi-responsiveness to pH, temperature and even ions. This type of SMP system may open another avenue for promoting the biomedical applications of SMPs in the fields of gene delivery, gene modification and gene therapy.

Therefore, we propose the molecular design of novel biocompatible SMPs based on DMAEMA. pDMAEMA generally shows a high transition temperature, and butyl acrylate (BA) is thus used to adjust the glass transition temperature, while chemical

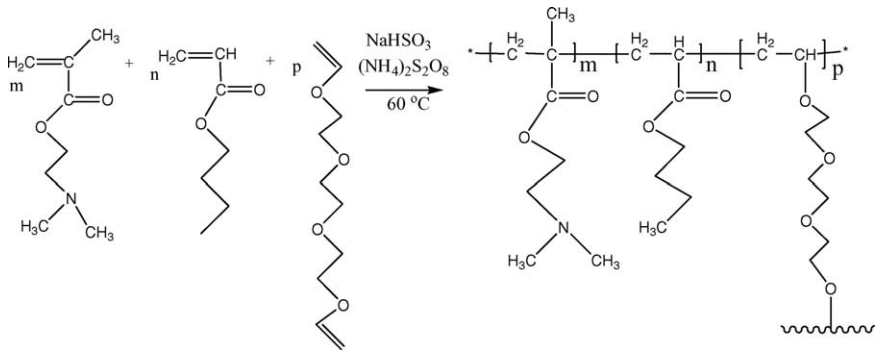

Scheme 1. Synthetic route of DMAEMA-co-BA-co-TDE copolymers. BA, butyl acrylate; DMAEMA, 2-(dimethylamino) ethyl methacrylate; TDE, tri(-ethylene glycol) divinyl ether.

cross-linking with tri(ethylene glycol) divinyl ether (TDE) endows the DMAEMA-co-BA-co-TDE copolymers with good shape memory functionality. This paper reports on the preparation of DMAEMA-co-BA-co-TDE copolymers. The structure, morphology and properties were investigated preliminarily by FT-IR, differential scanning calorimetry (DSC), thermogravimetric analysis (TGA) and DMA. In particular, the polymers' shape memory behaviour was studied carefully.

EXPERIMENTAL

Materials

Raw materials including 2-(dimethylamino) ethyl methacrylate (DMAEMA, analytic grade), butyl acrylate (BA, analytic grade), tri(ethylene glycol) divinyl ether (TDE, analytic grade), ammonium persulphate ($(NH_4)_2S_2O_8$, analytic grade) and sodium bisulphate ($NaHSO_3$, analytic grade) were all purchased from Aladdin (Shanghai, China) and used as received.

Preparation

A series of DMAEMA-co-BA-co-TDE copolymers were synthesized using soap-free emulsion polymerization. The synthetic route is presented in Scheme 1. The preparation of the copolymers was performed in a nitrogen-filled and mechanically stirred 500 ml three-neck flask. In a typical procedure, 65 ml deionized water, 0.17 g $NaHSO_3$ and 0.07 g $(NH_4)_2S_2O_8$ were first added into the flasks under vigorous stirring, followed by the addition of the raw materials DMAEMA, BA, and/or TDE according to each polymer's composition (Table I). Thereafter, the reaction temperature was increased to ~75°C, and 0.23 g $(NH_4)_2S_2O_8$ dissolved in 35 ml deionized water was dropped into the flask within 60 min. The reaction was performed hermetically at 75°C >5 h. Finally, water was evaporated from the resulting 20 wt % solution in a Teflon pan at 80°C for 24 h under continuous air flow and then under vacuum for another 24 h. For comparison, DMAEMA-co-BA copolymer (coded as DMAEMA-BA) and pDMAEMA were also synthesized directly using the same synthesis method described above. Samples of DMAEMA-co-BA-co-TDE copolymer were coded as DMAEMA-BA**-TDE, where "**" denotes the BA content.

Characterization

Attenuated total reflection Fourier transform infrared (ATR-FTIR) spectra were recorded with a Nicolet 760 FT-IR spectrometer equipped with an ATR accessory using a GeS crystal. Twenty-four scans at a resolution of 4 cm^{-1} were signal-averaged and stored as data files for further analysis.

The size of polymer micelles was investigated using a Zataplus Laser Scattering Particle Analyzer (Brookharen, USA). Each sample was measured at least five times, and the average size was recorded for analysis.

Static contact angle measurements were performed on a JC2000Y stable contact angle analyzer (China) at room temperature with distilled water as test liquid. With each specimen, the measurements were repeated at three different locations.

The weight percentages of C, H, and N of the samples were determined using a Vario EL III elemental analyzer (EA, Germany Elementar).

Table I. Compositions of DMAEMA-co-BA-co-TDE Copolymers

Samples	Content in Feed (wt %)			Elemental Composition (wt %)		
	DMAEMA	BA	TDE	N	C	H
pDMAEMA	100.00	0	0	-	-	-
DMAEMA-BA	86.00	14.00	0	6.57	56.52	8.965
DMAEMA-BA13-TDE	77.50	12.65	9.91	6.15	57.27	9.010
DMAEMA-BA15-TDE	74.85	15.27	9.91	6.05	58.04	8.962
DMAEMA-BA22-TDE	67.95	22.16	9.91	5.39	57.43	8.994
DMAEMA-BA29-TDE	60.50	29.59	9.91	5.21	57.26	8.881

BA, butyl acrylate; DMAEMA, 2-(dimethylamino) ethyl methacrylate; TDE, tri(ethylene glycol) divinyl ether.

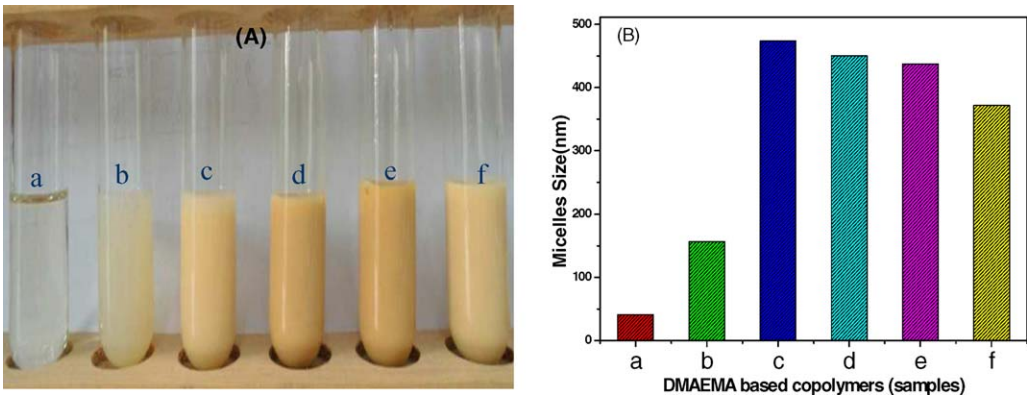

Figure 1. Images of the resulting solution and the micelle size of 2-(dimethylamino) ethyl methacrylate (DMAEMA)-based copolymers. [Color figure can be viewed in the online issue, which is available at wileyonlinelibrary.com.]

DSC testing was carried out by using a TA Q200 instrument with nitrogen as the purged gas. Indium and zinc standards were used for calibration. Samples were first heated from ⁻60°C to 150°C at a heating rate of 10°C/min and held at 150°C for 1 min and subsequently cooled to ⁻60°C at a cooling rate of 10°C/min; finally, a second heating scan from ⁻60°C to 150°C was performed.

TGA curves were recorded after drying at 100°C on a computer-controlled TA Instrument TG Q50 system under the following operating conditions: heating rate 10°C/min, temperature range 100–600°C, sample weight ~5.0 mg, and 60 ml/min N_2 flow, with film samples prepared in platinum crucibles. Three or four repeated readings (temperature and weight loss) were performed for the same TG curve, each composed of at least 15 points.

Modulus testing was carried out using a computer-controlled TA Instrument DMA800 system. Specimens were cut from a sample film with a thickness of 0.5 mm, and the distance between two clamps was 10 mm in the initial testing configuration. Specimens were analyzed at 1.0 Hz and a heating rate of 2.0 K/min.

The thermally induced shape-memory behaviour of the films was determined by cyclic thermo-mechanical analysis using a DMA800 instrument (tension clamp, controlled force mode) according to the procedure described in the literature.[20–22] The following test setups were used: (1) heating the sample to 95°C and equilibrating it for 35 min; (2) uniaxially stretching by ramping the applied force from 0.001 N to 1 N at a rate of 0.25 N/min; equilibration for 3 min; (3) fixing the strain by quickly cooling to 25°C or 0°C at a cooling rate of 10°C/min, followed by equilibration for 20 min; (4) unloading the external force to 0 N at a rate of 0.25 N/min; (5) reheating to 115°C or 125°C at a rate of 4°C/min and followed by equilibration for 25 min.

RESULTS AND DISCUSSIONS

Structure Analysis

In this experiment, the obtained pDMAEMA solution was a colourless, *transparent* watery solution, whereas the DMAEMA-co-BA copolymer solution as a micro-emulsion. In particular, the DMAEMA-co-BA-co-TDE copolymers were yellow emulsions, implying the formation of micelles [Figure 1(A)]. The formation of micelles was also confirmed by a Zataplus Laser Scattering Particle Analyzer. The size of the micelles in the DMAEMA-co-BA-co-TDE copolymer solution ranged from 371.4 nm to 473.6 nm, whereas the DMAEMA-co-BA copolymer solution formed micelles measuring only 157.0 nm [Figure 1(B)]. Moreover, the micelle size decreased with the increase in the BA content due to the increased hydrophobicity imparted by the BA segment in the DMAEMA-co-BA-co-TDE copolymers. Hydrophobicity of DMAEMA based copolymers was investigated with static water contact angle. The pDMAEMA polymers shows water contact angle of only 46.71°; While the DMAEMA-co-BA copolymer shows much higher water contact angle (above 66°) due to the copolymerization with BA segment. Moreover, the water contact angle also increases with the increase of BA content in the DMAEMA-co-BA-co-TDE copolymers (Figure 2). After drying, the resulting DMAEMA-co-BA-co-TDE copolymers could not be redissolved in water, DMF or THF. This finding indicates that chemical crosslinking was successfully achieved in the DMAEMA-co-BA-co-TDE copolymers. The hydrophobicity of BA segment and chemical crosslinking by

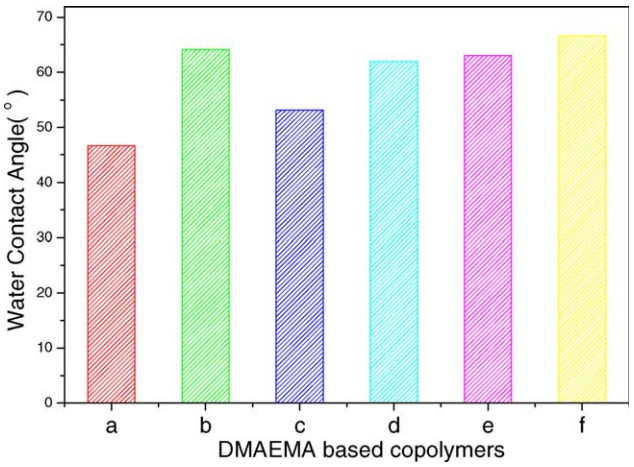

Figure 2. Water contract angle showing hydrophobicity of DMAEMA based copolymers. [Color figure can be viewed in the online issue, which is available at wileyonlinelibrary.com.]

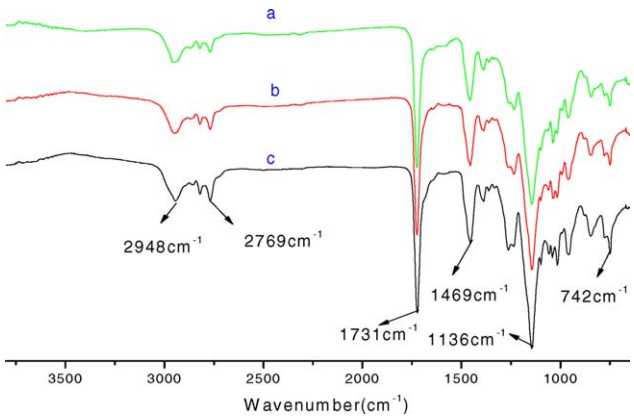

Figure 3. FT-IR spectra of DMAEMA copolymers. [Color figure can be viewed in the online issue, which is available at wileyonlinelibrary.com.]

TDE promote the formation of DMAEMA based copolymers micelles in aqueous solution.

The molecular structures of DMAEMA based copolymers were then investigated by ATR-FTIR. Figure 3 shows the FT-IR spectra of pDMAEMA and the DMAEMA-co-BA and DMAEMA-BA13-TDE copolymers. A strong absorbance peak attributed to C═O was observed at 1731 cm^{-1} in the pDMAEMA, DMAEMA-co-BA copolymer and DMAEMA-BA13-TDE copolymer solutions. A strong peak at 1469 cm^{-1} was also observed for all polymers, which could be attributed to the bending vibration of C—N bonds. In addition, bands attributed to $–CH_2$ and $\alpha–CH_3$ were detected at 2769 cm^{-1} to 2948 cm^{-1}, and the peak associated with wave vibrations belonging to the alkyl groups of the polymers also appeared at 742 cm^{-1}.[23] All of these findings demonstrate that pDMAEMA, DMAEMA-co-BA copolymer and DMAEMA-BA-TDE copolymer were successfully synthesized. The bulk elemental compositions of samples were further determined using a Vario EL Ⅲ elemental analyzer. The weight percentages of C, H, and N are provided in Table I. In particular, the N weight percentage increased with the DMAEMA content in the feed, whereas it decreased with the increase in the BA content in the DMAEMA-co-BA-co-TDE copolymer. These results thus confirm the successful copolymerization of DMAEMA with BA. Therefore, all of the DMAEMA-co-BA-co-TDE copolymers contained the functional group $–N(CH_3)_2$, which can be further quaternized to demonstrate antibacterial properties[24] or betainized to exhibit good biocompatibility.[25]

Thermal Properties

Thermal properties including the thermal phase transition and thermal stability of DMAEMA-co-BA-co-TDE copolymers were investigated by DSC and TGA. The second DSC curves demonstrate that all DMAEMA-co-BA-co-TDE copolymers formed an amorphous soft phase, without showing any trace of crystallization or melting. As the BA content increased, the glass transition temperature (T_g) shifted to lower temperatures (Figure 4). Ignoring temperature-based applications, this glass transition can be used to trigger shape recovery, particularly under chemical crosslinking conditions.[26] In addition, the TGA curves demonstrate that all DMAEMA-co-BA-co-TDE copolymers exhibited an initial decomposition temperature above 200°C, suggesting the formation of long carbon chains [Figure 5(A)]. Similarly to the pure pDMAEMA, the decomposition of the DMAEMA-co-BA-co-TDE copolymers is divided into two stages. The first stage may be associated with the decomposition of DMAEMA groups because the weight loss of pDMAEMA is much higher than that of DMAEMA-co-BA-co-TDE copolymers. The derivative thermogravimetry (DTG) curves also show that the pDMAEMA polymer exhibited the highest rate of decomposition [Figure 5(B)]. The second stage should belong to the decomposition of the polymer chain, as the decomposition of carbon chains requires high temperature. The results thus suggest that the decomposition of pDMAEMA and its copolymers began with the DMAEMA group due to its weak ester bonds (—O—C=O). This finding indicates that the thermal stability of DMAEMA-based polymers is greatly affected by this ester bond. That is, the thermal stability of DMAEMA-co-BA-co-TDE copolymers may be determined by the DMAEMA structure and content.

Dynamic Mechanical Properties

The thermal phase transitions of DMAEMA-co-BA-co-TDE copolymers were further investigated using DMA based on the values of the temperature-dependent modulus (E′) and tanδ (Figure 6). The E′ (T) curves [Figure 5(A)] show that all DMAEMA-co-BA-co-TDE copolymers and pDMAEMA exhibited high storage moduli in the glassy state, e.g., below 25°C, where the storage moduli decreased significantly around T_g. In particular, the pDMAEMA became too soft to measure properly above ≈130°C, suggesting that the samples possessed high molar masses and lacked sizeable crosslinking.[27] By contrast, the DMAEMA-co-BA-co-TDE copolymers showed higher rubber moduli above ≈120°C, confirming the formation of chemical crosslinks. In addition, the tanδ (T) curves [Figure 6(B)] corroborate the glass transition identified by DSC analysis (Figure 4). Pure pDMAEMA showed only one broad α-relax peak, belonging to the glass transition. After cross-linking the DMAEMA-co-BA-co-TDE copolymers, the appearance of more than two main relax peaks implied the existence of a microphase-separated structure. The DMAEMA-co-BA-co-TDE

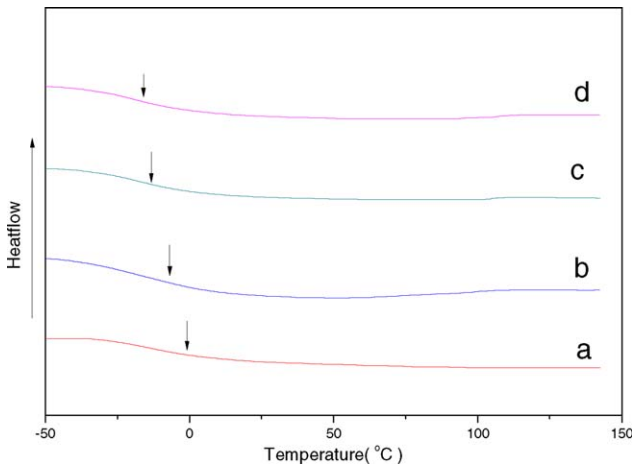

Figure 4. The second DSC curves of DMAEMA copolymer. [Color figure can be viewed in the online issue, which is available at wileyonlinelibrary.com.]

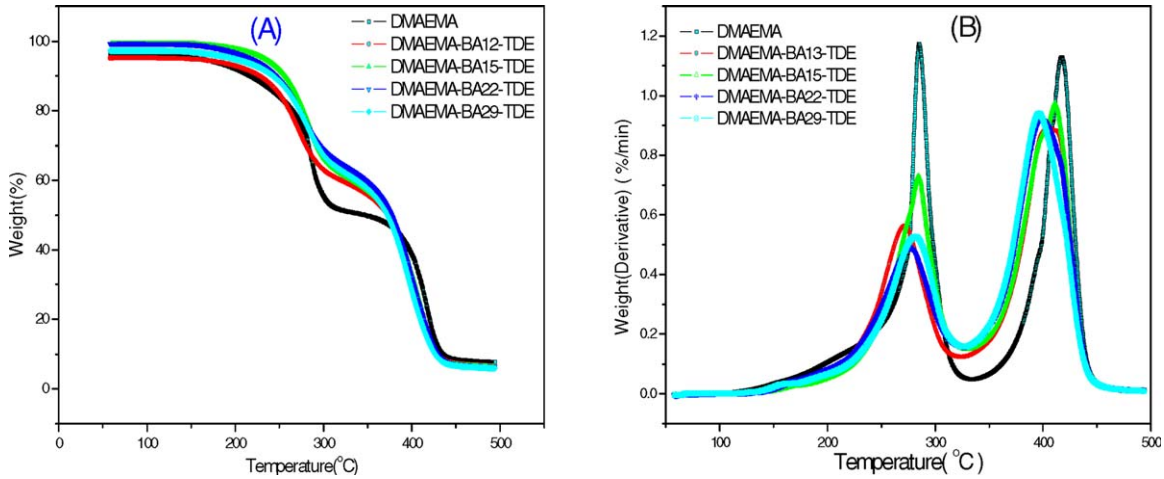

Figure 5. TG-DTG curves of DMAEMA copolymers with different BA content. TG-DTG: thermogravimetric-derivative thermogravimetry. [Color figure can be viewed in the online issue, which is available at wileyonlinelibrary.com.]

copolymers containing high BA content tend to show three different regimes. Below the temperature 50°C, the weak relax ascribed to the glass transition of BA–rich domains occurs, because the relax peak shifts to lower temperature range as the BA content increases, and no lower temperature relax is detected in pure pDMAEMA [Figure 6(B)]. The second relax detected above the temperature 110°C should be ascribed to the glass transition of DMAEMA-rich domains. As compared with the pure DMAEMA, the T_g of DMAEMA phase in the DMAEMA-co-BA-co-TDE copolymers has been improved greatly due to the chemical-crosslinking. The similarity of the changes around T_g from DMAEMA-BA12-TDE to DMAEMA-BA29-TDE also suggests that the chain dynamics themselves are mostly determined by the flexibility of chains and not by the extent of chemical crosslinking.

Shape Memory Properties

Based on the thermal properties and dynamic mechanical properties discussed above, a micro-phase-separated structure containing a reversible amorphous soft phase and the formation of chemical crosslinking both satisfied the structural requirements for exhibiting shape memory effects.[26] Thus, the thermally induced shape memory functionality of the samples was investigated. A qualitative test showed that the typical sample DMAEMA-BA15-TDE could be deformed from its original shape [Figure 7(A)] into a second shape [Figure 7(B)]. Upon heating, the fixed second shape began to recover at approximately 35°C [Figure 7(C–E)], and the temporary shape was recovered completely above 65°C [Figure 7(F)]. This process demonstrates that the DMAEMA copolymers have the capability to be fixed into a temporary shape and recover their original shape. Additionally, cyclic thermo-mechanical analysis further demonstrated that samples DMAEMA-BA15-TDE and DMAEMA-BA22-TDE both exhibited good shape fixity, reaching 100%. The sample DMAEMA-BA15-TDE showed ~90% shape recovery, whereas the sample DMAEMA-BA22-TDE showed <80% shape recovery (Figure 8). This result implies that a high BA content may destroy the samples' capacity for shape recovery. One possible

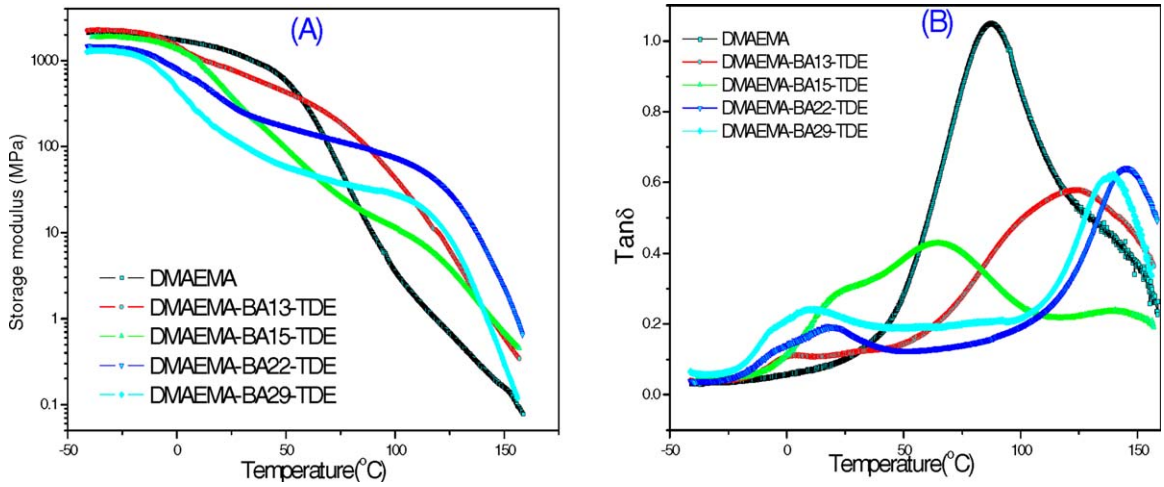

Figure 6. E′(T) and tanδ(T) curves of DMAEMA copolymers with different BA content. [Color figure can be viewed in the online issue, which is available at wileyonlinelibrary.com.]

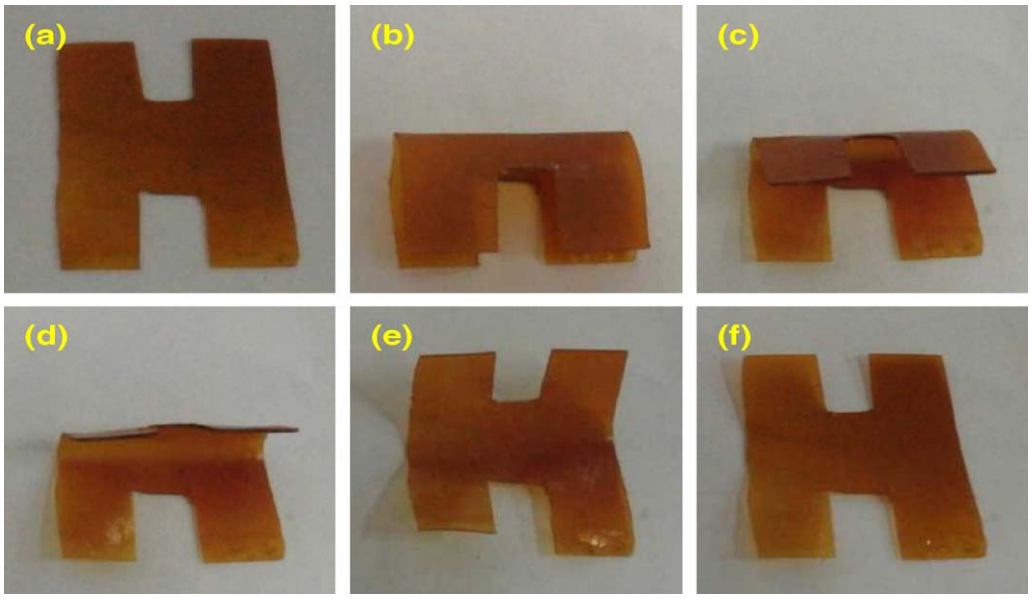

Figure 7. Shape recovery process of DMAEMA-BA15-TDE sample. [Color figure can be viewed in the online issue, which is available at wileyonlinelibrary.com.]

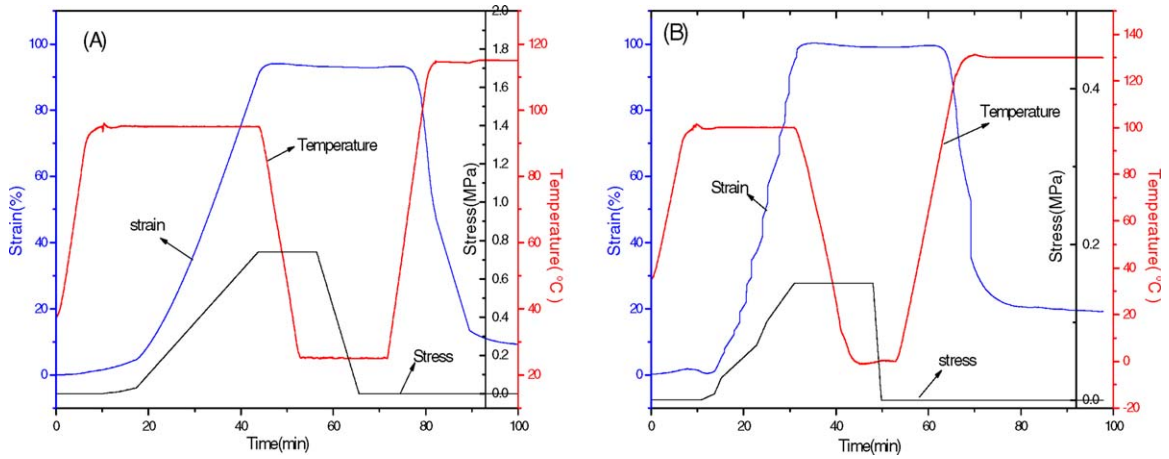

Figure 8. Cyclic thermo-mechanical curves. [Color figure can be viewed in the online issue, which is available at wileyonlinelibrary.com.]

reason is that the BA segment affects the mobility of polymer chains, as indicated by the tanδ(T) curves [Figure 6(B)]. The inherent reason should be further investigated. In contrast, both qualitative and quantitative tests confirmed that DMAEMA-co-BA-co-TDE copolymers can be used as shape memory materials by adjusting the BA content through chemical crosslinking. Considering the basic biomaterials properties of DMAEMA copolymers, including antibacterial activity and biocompatibility,[24,25] DMAEMA-co-BA-co-TDE copolymers are good candidates for smart biomaterials applications.

CONCLUSIONS

This communication reports the preparation of DEMAEMA-co-BA-co-TDE copolymers demonstrating shape memory effects. Structural analysis confirms that DMAEMA-co-BA-co-TDE copolymers form micelles in solution by chemical crosslinking and hydrophobic interactions. After drying, the resulting polymer film contains the functional group $-N(CH_3)_2$, which can be used in further biomaterials applications. Experiments analyzing thermal properties and dynamic mechanical properties demonstrate that DEMA-BA-TDE copolymers form a micro-phase-separated structure containing a reversible amorphous soft phase and chemical crosslinking. Finally, both qualitative and quantitative tests confirm that DMAEMA-co-BA-co-TDE copolymers can be used as shape memory materials by adjusting the BA content. Considering the basic biomaterials properties of DMAEMA copolymers, DMAEMA-co-BA-co-TDE copolymers are thus proposed as good candidates for smart biomaterials applications.

ACKNOWLEDGMENTS

This work was financially supported by the National Natural Science Foundation of China (grant No. 21104045), the Special Research

Foundation of Shenzhen Oversea High-level Talents for Innovation and Entrepreneurship (Grant No. KQCX20120807153115869), and the Nanshan District Key Lab for Biopolymers and Safety Evaluation (No.KC2014ZDZJ0001A).

REFERENCES

1. Chen, S.; Hu, J.; Yuen, C. M.; Chan, L. *Mater. Lett.* **2009**, *63*, 1462.
2. Hu, J.; Chen, S. *J. Mater. Chem.* **2010**, *20*, 3346.
3. Wong, Y.; Kong, J.; Widjaja, L. K.; Venkatraman, S. S. *Sci. China Chem.* **2014**, *57*, 476.
4. Small, W.; Singhal, P.; Wilson, T. S.; Maitl, D. J. *J. Mater. Chem.* **2010**, *20*, 3356.
5. Yi, Z.; Zhu, L. P.; Zhao, Y. F.; Wang, Z. B.; Zhu, B. K.; Xu, Y. Y. *J. Membrane Sci.* **2014**, *463*, 49.
6. Sui, K.; Shan, X.; Gao, S.; Xia, Y.; Zheng, Q.; Xie, D. *J. Polym. Sci. Polym. Chem.* **2010**, *48*, 2143.
7. Popescu, M. T.; Tsitsilianis, C.; Papadakis, C. M.; Adelsberger, J.; Balog, S.; Busch, P.; Hadjiantoniou, N. A.; Patrickios, C. S. *Macromolecules* **2012**, *45*, 3523.
8. Guo, W.; Wang, T.; Tang, X.; Zhang, Q.; Yu, F.; Pei, M., *J. Polym. Sci. Polym. Chem.* **2014**, *52*, 2131.
9. Bertrand, O.; Poggi, E.; Gohy, J. F.; Fustin, C. A. *Macromolecules* **2014**, *47*, 183.
10. Ivan Melendez-Ortiz, H.; Peralta, R. D.; Bucio, E.; Zerrweck-Maldonado, L., *Polym. Eng. Sci.* **2014**, *54*, 1625.
11. Arslan, H.; Pfaff, A.; Lu, Y.; Stepanek, P.; Mueller, A. H. E. *Macromol. Biosci.* **2014**, *14*, 81.
12. Li, Y.; Liu, T.; Zhang, G.; Ge, Z.; Liu, S. *Macromol. Rapid Comm.* **2014**, *35*, 466.
13. Lee, H. C.; Hsueh, H. Y.; Jeng, U. S.; Ho, R. M. *Macromolecules* **2014**, *47*, 3041.
14. Schepelina, O.; Poth, N.; Zharov, I. *Adv. Funct. Mater.* **2010**, *20*, 1962.
15. Zhu, L. J.; Zhu, L. P.; Zhao, Y. F.; Zhu, B. K.; Xu, Y. Y. *J. Mater. Chem. A* **2014**, *2*, 15566.
16. Han, X.; Feng, J.; Dong, F.; Zhang, X.; Liu, H.; Hu, Y. *Mol. Phys.* **2014**, *112*, 2046.
17. Zhang, Q.; Tang, X.; Wang, T.; Yu, F.; Guo, W.; Pei, M. *RSC Adv.* **2014**, *4*, 24240.
18. Perbone de Souza, J. C.; Naves, A. F.; Florenzano, F. H. *Colloid Polym. Sci.* **2012**, *290*, 1285.
19. Qian, Y.; Zha, Y.; Feng, B.; Pang, Z.; Zhang, B.; Sun, X.; Ren, J.; Zhang, C.; Shao, X.; Zhang, Q.; Jiang, X. *Biomaterials* **2013**, *34*, 2117.
20. Kasi, R. M.; Ahn, S. K.; Deshmukh, P. *Macromolecules* **2010**, *43*, 7330.
21. Xie, T. *Nature* **2010**, *464*, 267.
22. Luo, Y.; Guo, Y.; Gao, X.; Li, B. G.; Xie, T. *Adv. Mater.* **2013**, *25*, 743.
23. Zhou, W.; Liu, H.; Ye, H.; Cui, H.; Wang, R.; Li, J.; Zhang, X. *Powder Technol.* **2013**, *249*, 1.
24. Yu, H.; Fu, Y.; Li, G.; Liu, Y. *holzforschung* **2013**, *67*, 455.
25. Lowe, A. B.; Billingham, N. C.; Armes, S. P. *Macromolecules* **1999**, *32*, 2141.
26. Hu, J. L; Chen, S. J. *J. Mater. Chem.* **2010**, *20*, 3346.
27. Frisch, H. L. *Polym. Eng. Sci.* **1980**, *20*, 2.